Determination of the experimental equilibrium structure of solid nitromethane using path-integral molecular dynamics simulations

Determination of the experimental equilibrium structure of solid nitromethane using path-integral molecular dynamics simulations

Anthony M. Reilly, Scott Habershon, Carole A. Morrison, and David W. H. Rankin

Citation: J. Chem. Phys. **132**, 094502 (2010); doi: 10.1063/1.3335817
View online: http://dx.doi.org/10.1063/1.3335817
View Table of Contents: http://jcp.aip.org/resource/1/JCPSA6/v132/i9
Published by the AIP Publishing LLC.

Determination of the experimental equilibrium structure of solid nitromethane using path-integral molecular dynamics simulations

Anthony M. Reilly,[1] Scott Habershon,[2] Carole A. Morrison,[1,a)] and David W. H. Rankin[1]
[1]*School of Chemistry, University of Edinburgh, West Mains Road, EH9 3JJ Edinburgh, United Kingdom*
[2]*Department of Chemistry, Physical and Theoretical Chemistry Laboratory, University of Oxford, South Parks Road, OX1 3QZ Oxford, United Kingdom*

(Received 15 December 2009; accepted 4 February 2010; published online 2 March 2010)

Path-integral molecular dynamics (PIMD) simulations with an empirical interaction potential have been used to determine the experimental equilibrium structure of solid nitromethane at 4.2 and 15 K. By comparing the time-averaged molecular structure determined in a PIMD simulation to the calculated minimum-energy (zero-temperature) molecular structure, we have derived structural corrections that describe the effects of thermal motion. These corrections were subsequently used to determine the equilibrium structure of nitromethane from the experimental time-averaged structure. We find that the corrections to the intramolecular and intermolecular bond distances, as well as to the torsion angles, are quite significant, particularly for those atoms participating in the anharmonic motion of the methyl group. Our results demonstrate that simple harmonic models of thermal motion may not be sufficiently accurate, even at low temperatures, while molecular simulations employing more realistic potential-energy surfaces can provide important insight into the role and magnitude of anharmonic atomic motions. © *2010 American Institute of Physics*.
[doi:10.1063/1.3335817]

I. INTRODUCTION

Diffraction techniques represent one of the most robust methods for determining molecular structures. They can be applied to a wide array of systems, ranging from crystallized proteins to isolated molecules in the gas phase. In addition, diffraction studies can also be used to investigate the effects of temperature and pressure on structure at the atomic scale.[1] However, when comparing structures obtained by diffraction experiments and theoretical calculations, it is important to remember that the experimental structures represents an average over atomic thermal motion, whereas theory usually provides a "zero temperature" equilibrium structure devoid of such effects, including zero-point energy (ZPE) effects.

It has long been a goal of structural scientists to correct experimentally determined, time-averaged structures in order to derive the equilibrium structure at the minimum of the potential-energy surface. The need to correct structures arises from the anharmonic nature of vibrational motions. The majority of solid-state diffraction studies treat thermal motion as being harmonic in nature, modeling each atom's dynamics with monovariate or trivariate Gaussian probability density functions (PDFs). For the general trivariate case, this requires the definition of six additional parameters for each atom, representing the six unique elements, U_{ij}, of the 3×3 covariance matrix defining the harmonic motion. Specifically, diagonal terms, U_{ii}, represent the variance or extent of thermal motion, while the off diagonals, U_{ij}, are the covariances that determine the orientation of the distribution relative to the crystallographic axes. Collectively, the elements U_{ij} are referred to as the anisotropic displacement parameters (ADPs).

Although a harmonic model can describe the major effects of thermal motion on diffraction intensities, it has long been known that such models can lead to inconsistent geometries when the atoms and molecules undergo librational or anharmonic motion.[2] As a result, a number of different approaches have been developed to address this problem. For example, the *a posteriori* approach of the translational/librational/screw (TLS) method[3] corrects bonded distances in harmonically refined structures for the effects of librational motion. There also exist several methods that use anharmonic PDFs to model the motional asymmetry;[4] however, the use of anharmonic PDFs (or their equivalent in reciprocal space, the Debye–Waller factor) has been limited by the large number of extra parameters required. A further complication arises because the typical form of the structure factor used to model crystallographic data sets assumes that each atom is independent from the other atoms in the system. This approximation suggests that information on the global potential-energy surface (the minimum of which is the desired equilibrium structure) is not strictly available from a single diffraction experiment.[5]

We have recently outlined a new method to determine equilibrium structures of solids[6] and gases[7] from experimental diffraction data. This approach uses molecular dynamics (MD) simulations to determine the time-averaged structure of a molecule or crystal, including the appropriate thermal motion. The difference between this time-averaged structure and the theoretical equilibrium structure obtained by energy minimization should represent a suitable correction to the

a)Electronic mail: carole.morrison@ed.ac.uk.

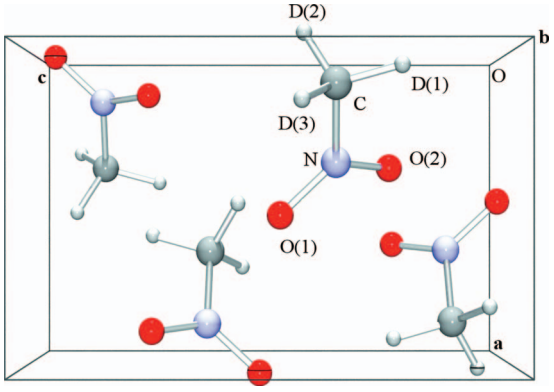

FIG. 1. Crystal structure of d_3-nitromethane with atom labels and numbers. The space group is $P2_12_12_1$ and the unit cell parameters are a=5.185 Å, b=6.237 Å, and c=8.507 Å at 15 K (Ref. 8).

experimental time-averaged structure, thereby allowing one to derive the experimental equilibrium structure. In the present work, we expand on our initial proof-of-concept study of phase I ammonia[6] and apply this method to study the crystal structure of nitromethane, CH_3NO_2, at a range of temperatures.

Nitromethane crystallizes in the $P2_12_12_1$ space group with four molecules in the unit cell, as shown in Fig. 1.[8] The methyl group of nitromethane has a low barrier to rotation ($\simeq$2.8 kJ mol^{-1}),[9] which results in large-amplitude motions of the hydrogen atoms around the axis of the C–N bond. This motion makes the H atoms appear to be closer to their centroid and results in substantially shorter C–H distances than would be expected. This phenomenon is often observed in methyl groups in many crystal structures, even in cases where the methyl group rotation is hindered.[10] Nitromethane is therefore a model system for one of the most common manifestations of anharmonic thermal motion in crystallography.

Many of the structural and dynamical studies previously reported for nitromethane have focused on the thermal motion of the methyl group. All three neutron diffraction studies of deuterated nitromethane (d_3-nitromethane) have attempted to use theoretical methods to correct the C–D distances for the effects of libration and all were performed at low temperatures (4.2–78 K) to minimize the amplitude of this motion.[8,11,12] Other studies have applied neutron scattering techniques to investigate the potential-energy barrier governing methyl group rotation.[13,14]

More recently, interest in nitromethane has focused on its role as an energetic material. A number of experimental studies of its behavior under high pressure[15,16] have been made, as have theoretical investigations of its physical properties.[17] Many of these simulations have applied the empirical force-field developed by Sorescu *et al.*[18] This force field has been used in the simulations presented here as it has been widely applied to both solid-state and liquid nitromethane and has been demonstrated to reproduce key physical properties such as the thermal expansion and bulk modulus. Normally, it would be preferable to use an advanced electronic-structure method such as density functional theory (DFT) to describe the potential energy surface but a previous DFT study of nitromethane showed that the lack of dispersion forces in mainstream functionals limits the accuracy of calculated cell vectors and other properties.[19] Recent work,[20] however, has shown that Grimme-type dispersion corrections[21] improve the DFT modeling of nitromethane. Nevertheless our choice of empirical potentials has allowed us to simulate larger supercells and to acquire longer trajectories than would be possible using DFT-based modeling approaches. Crucially, the computational speed of empirical force fields has permitted us to perform path-integral MD (PIMD) simulations. We find that path-integral simulations, which allow one to account for nuclear quantum effects such as tunneling and ZPE conservation, are essential in describing low-temperature experimental data, as noted previously for the case of solid helium at temperatures down to 5 K.[22]

The purpose of the work described in this paper was to use MD simulations to study the structure of nitromethane over a range of temperatures in order to investigate the temperature dependence of the anharmonic motion, structural corrections, and ADPs. This work shows the potential of classical MD and quantum PIMD simulations in determining equilibrium structures and also in providing useful model data sets for understanding the effects of anharmonic thermal motion in crystallography. In the remainder of this paper, Sec. II outlines our computational approach, Sec. III A assesses the importance of nuclear quantum effects in the atomic motion, while in Sec. III B we use previous experimental structures at 4.2 and 15 K to determine the experimental equilibrium structure of nitromethane. Finally, Sec. III C compares different models of thermal motion to the results obtained from quantum PIMD simulations.

II. COMPUTATIONAL METHODS

A. Structural definitions

In order to aid later discussion, it will be useful to define a number of different positional parameters in the theoretical and experimental crystal structures. Here, three-dimensional positions will be denoted $\mathbf{r}$, and interatomic distances, bond angles, and torsion angles will be denoted r, $\angle$, and ϕ, respectively.

Parameters determined from the theoretical equilibrium (minimum energy) geometries are referenced with a subscript "e" (e.g., $\mathbf{r}_e$), and time-averaged values determined in MD simulations are denoted $\mathbf{r}_{ave}^{MD}$. The experimental time-averaged values are denoted $\mathbf{r}_{ave}^{exp}$. The equilibrium geometries obtained after applying the structural corrections determined by MD simulations to the experimental data are denoted $\mathbf{r}_e^{MD}$. These four different structures are clearly related by

$$\mathbf{r}_e^{MD} = \mathbf{r}_{ave}^{exp} + (\mathbf{r}_e - \mathbf{r}_{ave}^{MD}) = \mathbf{r}_{ave}^{exp} + \Delta\mathbf{r}_{MD}. \quad (1)$$

We note that the corrections are applied in terms of fractional coordinates to avoid complications arising due to different theoretical and experimental lattice vectors. Experimental equilibrium bond lengths and angles were derived from the corrected $\mathbf{r}_e^{MD}$ coordinates. The use of vectorial MD corrections means that the experimental equilibrium structure can

be obtained in a simple and consistent manner; there may be some error in this approach due to the experimental and theoretical systems having slightly different orientations relative to the lattice vectors, but we find that these are typically of the same order of magnitude as the experimental uncertainty.

B. MD simulations

MD simulations of d_3-nitromethane were carried out using the empirical force-field of Sorescu *et al.*[18] Here, intermolecular dispersion interactions were described using a Buckingham potential with parameters originally developed for the energetic material hexahydro-1,3,5-trinitro-1,3,5-*s*-triazine.[23] Electrostatic interactions between fixed partial charges on each atom were calculated by standard Ewald summation.[24] The intramolecular potential-energy surface used Morse potentials to represent bond stretches, while angle bends were treated using harmonic functions.[25] The O–N–C–D torsions were modeled as having threefold symmetry (in the absence of the crystal field) using a cosine function,

$$V(\phi) = V_0[1 + \cos(3\phi - \delta)], \tag{2}$$

where δ adjusts the position of the torsional energy minimum. In the original paper,[18] values of $\pm 90°$ were used, but initial classical MD simulations suggested that values of $\pm 70°$ provide better agreement with the experimental 15 K torsion angles of Jeffrey *et al.*[8] In quantum PIMD simulations, this agreement worsens slightly, but the time-averaged 15 K values of 156°, −84°, and 36° for the O(1)–N–C–D(1–3) torsions are still closer to the experimental values (151°, −89°, and 30°) than the values obtained with the original force field (161°, −78°, and 42°). As we expect thermal motion to affect the experimental values, we only aim to be close enough to obtain valid corrections, not absolute agreement.

In all calculations, we employed periodic boundary conditions using the minimum-image convention[24] and we used a simulation cell comprising $5 \times 4 \times 3$ unit cells (containing 240 nitromethane molecules). A cell of this size is roughly cubic and allows a cutoff distance of 10 Å for short-range interactions, as used in previous simulations.[17,18,26]

Classical MD simulations at constant *NVT* were performed at several temperatures ranging from 4.2 to 228 K. Sorescu *et al.* determined time-averaged lattice constants at a number of temperatures using *NPT* simulations. These lattice constants were either used for the equivalent *NVT* simulations in our work or, where no *NPT* simulation had been performed, data from adjacent temperatures were used to estimate lattice vectors assuming linear expansion of the cell. The velocity-verlet algorithm was used to integrate the equation of motion with a time step of 0.5 fs. An Andersen thermostat[27] was used to ensure correct thermal sampling. The simulated systems were initially equilibrated for 0.5 ps (longer equilibration times made no difference to our calculation results), after which configurational data was sampled every tenth step during a subsequent 20 ps ($T \leq 78$ K) or 30 ps ($T \geq 78$ K) trajectory.

Quantum PIMD simulations[28,29] were run at the same temperatures and using the same cell sizes as the classical MD simulations. The equations of motion for the ring-polymer system were integrated with a time step of 0.5 fs using a symplectic integrator employing alternating external force and free ring-polymer evolution steps. While the use of a classically determined cell size is likely to result in a non-ambient pressure in the PIMD simulations, it allows direct comparison of the quantum and classical results.

PIMD simulations at temperatures as low as 4.2 K require very large Trotter dimensions, or beads, P.[30] To increase the speed of the simulations, the ring-polymer contraction method was employed;[31,32] this method exploits the different characteristic spatial variations of the intramolecular and intermolecular potentials in order to minimize the number of ring-polymer beads without compromising the accuracy of the calculation. In our calculations at 4.2 K, we used 150 beads to describe intermolecular interactions and 500 beads to describe intramolecular interactions; these values were decreased accordingly when performing PIMD simulations at higher temperatures. Again, an Andersen thermostat was employed to ensure correct thermal sampling and nonergodicity in the PIMD simulation, and the full P-bead configurations of the system were used to calculate configurational properties every tenth time step.

Equilibrium geometries ($\mathbf{r}_e$) for each set of lattice vectors were determined using a steepest-descents approach starting from the experimental 15 K fractional coordinates. To ensure that the initial configuration did not result in a false minimum, an annealing MD simulation, in which the temperature was gradually lowered from 100 to 0 K, was carried out for the 15 K lattice vectors, with the result being identical to that obtained from the steepest-descents calculation. These equilibrium structures represent the system at rest but with finite-temperature lattice vectors. The expansion (or contraction) of the lattice is governed by thermal motion and the estimation of the equilibrium lattice vectors could be made by extrapolation of multitemperature experimental data to 0 K. In the present work, where the aim is to demonstrate that MD simulations can provide reasonable corrections to crystallographic data sets, we have simplified our computational approach by using the finite-temperature lattice vectors.

C. Trajectory analysis

The theoretical mean position, $\mathbf{r}_a$, of each atom was calculated during each classical or PIMD simulation using the full space group and supercell symmetry,

$$\mathbf{r}_a = (\overline{u_1}, \overline{u_2}, \overline{u_3}), \tag{3}$$

$$\overline{u_i} = \frac{1}{N \times S} \sum_{n=1}^{N} \sum_{j=1}^{S} u_{i,j,n} = \langle u_i \rangle, \tag{4}$$

where N is the total number of time steps in the sample, S is the total number of symmetry-equivalent atoms in the supercell, and $u_{i,j,n}$ is the value of the ith component of the position of atom j at time step n. The variances and covariances of each atomic position are given by

$$\sigma_{ij}^2 = \langle (u_i - \overline{u_i})(u_j - \overline{u_j}) \rangle = \langle \Delta u_i \Delta u_j \rangle, \quad (5)$$

where diagonal elements give the variances, σ_{ii}^2, and off-diagonal elements gives the covariances, σ_{ij}^2. The numerical evaluation of the mean and variances yields the true anharmonic mean and variance, while the Gaussian approximation commonly used in crystallographic calculations gives the corresponding harmonic values. At high temperatures, there may be appreciable differences between these quantities but for comparison with low-temperature experimental data performed here, the numerical covariance matrix should approximate the experimental ADPs sufficiently,

$$\sigma_{ij}^2 \approx U_{ij}. \quad (6)$$

For PIMD simulations with $P > 1$ ring-polymer beads, each bead was correctly included in the calculation of these averages so that $N \times S \times P$ data points were collected for each atom. Sampling uncertainties were estimated using the central limit theorem.[24]

The numerical PDFs were determined by binning the positions adopted by the atoms. As the methyl group rotates (even at very low temperatures), the D-atom indices were assigned at each time step by determining the dihedral angle of each D atom relative to the equilibrium O(1)–N–C fragment.

III. RESULTS AND DISCUSSION

A. Role of nuclear quantum effects

Comparing classical MD and quantum PIMD simulations of d_3-nitromethane allows us to assess the role of nuclear quantum effects, namely tunneling and ZPE, in the calculated ADPs and molecular structural parameters. This comparison also allows us to assess when classical MD simulations are not sufficient to model the structural properties accurately. Quantum effects are expected to be particularly important at the low temperatures studied here and for the properties associated with the light deuterium atoms. This is supported by previous lattice dynamics studies,[33] which have shown that quantum-mechanical effects can be important when simulating ADPs. Finally, it is important to bear in mind that the PIMD simulations give *exact* quantum-mechanical configurational properties for a given empirical force field.

The temperature dependence of the C and D(1) atom variances, as determined in classical MD and PIMD simulations, are shown in Fig. 2. As expected, the quantum ADPs level out as the temperature approaches 0 K, following the trend of a quantum harmonic oscillator, while the classical values fall to zero. The high-temperature deviations from harmonic oscillator behavior will be discussed more in Sec. III C. By 78 K, the classical D-atom ADPs are 80% of the quantum value, rising to 95% by 228 K. The remaining quantum contribution arises from the high-frequency internal degrees of freedom, such as C–D stretching motions. For the C atom, agreement at 228 K between the classical and quantum simulations is much better as a result of the heavier mass. We find that the shapes and orientations of the calculated atomic position distributions in classical and quantum

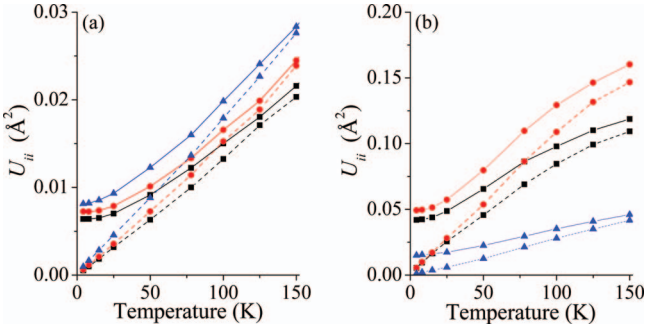

FIG. 2. Quantum (solid lines) and classical (dashed lines) U_{11}, U_{22}, and U_{33} values of (a) the C atom and (b) the D(1) atom at temperatures ranging from 4.2 to 150 K. Squares are U_{11} values, circles are U_{22} values, and triangles are U_{33} values.

simulations are quite similar, suggesting that classical simulations are useful for at least a qualitative analysis of the thermal motion. At lower temperatures, we find that the calculated ellipsoids begin to deviate, as suggested by Fig. 2. In particular, we find that the ratios of the variances along different axes are altered, with the longest principal axis of the PDF being better represented by the classical approximation than the shorter axes.

The differences between the quantum and classical descriptions of thermal motion have a significant effect on the resulting structural corrections. At very low temperatures, there is hardly any thermal motion in the classical simulation and therefore only a small correction. In contrast, the delocalization of the atomic distribution in the quantum simulations results in significantly different structural corrections. For example, at a temperature of 4.2 K, we find that the classical correction to the bond length C–D(1) is $\Delta r_{\mathrm{cl}} = 0.003$ Å, whereas the correction determined in the quantum PIMD simulation is $\Delta r_{\mathrm{qm}} = 0.021$ Å. This is a clear demonstration of the role of quantum fluctuations in the crystal structure at low temperatures. In keeping with Fig. 2, raising the temperature brings the classical and quantum corrections closer together. For example, at 78 K, the classical correction to the same bond length is $\Delta r_{\mathrm{cl}} = 0.054$ Å, whereas the PIMD value is $\Delta r_{\mathrm{qm}} = 0.059$ Å.

Although PIMD simulations give the exact quantum-mechanical configurational properties, they are around a factor of P times more expensive than the corresponding classical MD simulation. (This scaling comes from the fact that one must calculate the force acting on each of the P ring-polymer beads independently.) Although the ring-polymer contraction scheme[31,32] helps to alleviate this problem, it is worth considering whether the quantum nuclear effects can be successfully modeled by other, more approximate, methods. Here, we compare the results of PIMD simulations to those determined by the Feynman–Hibbs (FH) method.[28,34,35]

The FH method employs a quasiclassical interaction potential to account for the effects of delocalization of the quantum particles. Here, the classical potential for a particle, $V(\mathbf{r})$, is replaced by an effective potential,[28,34,35]

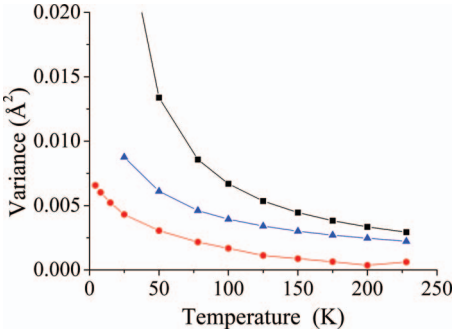

FIG. 3. Plot of $\frac{2}{3}r^2_{G,\ free}$ (squares), $\frac{2}{3}r^2_G$ (triangles), and ΔU_{eq} (circles) for the carbon atom in d_3-nitromethane at temperatures from 4.2 to 228 K.

$$V_{\text{eff}}(\mathbf{r}_c) = \frac{1}{\sqrt{8\pi^3\Delta r^2}}\int_{-\infty}^{\infty} V(\mathbf{r}_c+\mathbf{r})\exp\left(\frac{-\mathbf{r}^2}{2\Delta r^2}\right)d\mathbf{r}, \tag{7}$$

where Δr^2 is related to the free-particle radius-of-gyration, $r_{G,\ free}$, and the thermal wavelength, $\Lambda(T)$,[34,36]

$$\Delta r^2 = \frac{\Lambda(T)^2}{12\pi} = \frac{2}{3}r^2_{G,\ free} = \frac{\beta\hbar^2}{6m}, \tag{8}$$

where $\beta = 1/k_bT$ and m is the mass of the particle.

Equations (7) and (8) suggest an approximate approach to correcting classical simulation data for the effects of quantum-mechanical fluctuations. We may simply convolute structural properties determined in a classical calculation with an appropriate isotropic Gaussian function to account for the effects of quantum delocalization. This approach has been applied previously by Voth,[34] who showed that a quasiclassical probability density can be written as a convolution of the classical density and a Gaussian with a width of $\frac{2}{3}r^2_{G,\ free}$, where $r_{G,\ free}$ is the free ring-polymer radius of gyration at the simulation temperature. This simple FH approach predicts that the isotropic displacement parameter U_{eq} is given by

$$U^{FH}_{eq} = \tfrac{2}{3}r^2_{G,\ free} + U^{cl}_{eq}. \tag{9}$$

where U^{cl}_{eq} is the classical isotropic displacement parameter. Both the classical and quantum U_{eq} values can be calculated from the appropriate classical or path-integral MD simulation

$$U^{MD}_{eq} = \tfrac{1}{3}(U_{11}+U_{22}+U_{33}). \tag{10}$$

Comparing the predicted U^{FH}_{eq} to the PIMD simulated quantum U_{eq} values clearly gives a way of assessing whether the simple FH post-processing approach is appropriate for correcting a classical MD simulation for the influence of nuclear quantum effects.

Figure 3 shows the predicted isotropic displacement parameters arising as a result of quantum fluctuations, as calculated by the FH approach and by PIMD simulations at several temperatures. For this analysis, we have only considered the carbon atom because the lighter deuterium atoms are likely to undergo tunneling, which would skew the results of this comparison. The plot shows that $\frac{2}{3}r^2_{G,\ free}$ is much larger than the difference between the classical and quantum U_{eq} values at all temperatures. This indicates that the FH method overestimates the quantum swelling effect. Structural parameters calculated using this approach would therefore be in error too. This is perhaps not that surprising, as the free-particle radius of gyration is unlikely to be suitable for solid-state simulations, where the influence of the intermolecular interactions compresses the ring polymer and decreases the radius of gyration.

To improve the simple FH model, we could use the actual radius of gyration, r^2_G, of the carbon atom ring polymer, as determined in a short PIMD simulation. As shown in Fig. 3, we find that this approach certainly improves upon the estimate of the simple FH model, bringing the calculated U^{FH}_{eq} into better agreement with the exact PIMD results. However, our results suggest that, at least in the case of low-temperature crystalline solids like nitromethane, the full PIMD calculation provides the best route to including the contribution of nuclear quantum effects in calculated structural properties.

B. Comparison with previous experimental data sets

1. Single-crystal neutron diffraction at 15 K

As detailed in Sec. I, nitromethane has been studied a number of times using neutron and x-ray diffraction with an emphasis on correcting for thermal motion effects. Single-crystal neutron diffraction studies have been limited to the work of Jeffrey *et al.*[8] at 15 K. Their study determined positions and ADPs to a good degree of precision. Table I gives their experimental ADPs alongside our theoretical (PIMD) values. The agreement between the two sets of ADPs is quite good, with many of the displacement parameters being within 3σ of each other.

The good agreement between the experimental and theoretical ADPs means that the differences between the theoretical time-averaged (r^{MD}_{ave}) and equilibrium structures (r_e) should provide suitable positional corrections for the experimental structure. Even at temperatures as low as 15 K, these corrections are sizeable, ranging in magnitude from 0.021 Å for the N atom to 0.115 Å for D(1). The refinement of Jeffrey *et al.*[8] employed a segmented rigid-body TLS model,[37] in which the CNO_2 and CD_3 were treated as rigid fragments, to correct bond lengths for librational effects. In addition, an anharmonic distance correction was applied to the C–D distances to correct for bond-lengthening effects due to the anharmonicity of the bond-stretching motion. The TLS distance corrections therefore provide a useful benchmark for the MD-corrected values and the comparison is presented in Table II. For the heavy-atom bond lengths, we calculate quite small corrections, which are comparable to the experimental uncertainties. Our calculated corrections are of the same magnitude but opposite in sign to the TLS corrections. This probably arises because the experimental TLS corrections for the heavy-atom distances neglect the Morse contributions that result in longer experimental bonds. For the C–D distances, both methods determine large corrections of approximately 0.015–0.02 Å. The agreement between the two methods is not that surprising because, at low temperatures, the "harmonic" librational effects, which the TLS method deals

TABLE I. Experimental (Ref. 8) and theoretical ADPs (in Å^2) for d_3-nitromethane at 15 K.

		U_{11}	U_{22}	U_{33}	U_{12}	U_{23}	U_{31}
C	Expt.	0.0059(3)	0.0074(3)	0.0103(3)	0.0015(2)	−0.0005(2)	−0.0005(2)
	PIMD	0.0065(1)	0.0074(1)	0.0086(1)	0.0019(1)	−0.0004(1)	−0.0009(1)
N	Expt.	0.0047(2)	0.0055(2)	0.0074(2)	0.0006(2)	0.0000(2)	0.0002(2)
	PIMD	0.0048(1)	0.0050(1)	0.0058(1)	0.0005(1)	−0.0002(1)	0.0001(1)
O(1)	Expt.	0.0064(3)	0.0091(3)	0.0100(3)	0.0008(3)	0.0001(3)	−0.0021(3)
	PIMD	0.0072(1)	0.0099(1)	0.0086(1)	0.0010(1)	0.0006(1)	−0.0023(1)
O(2)	Expt.	0.0093(3)	0.0084(3)	0.0108(3)	0.0012(3)	−0.0037(3)	0.0003(3)
	PIMD	0.0104(1)	0.0096(1)	0.0089(1)	0.0020(1)	−0.0036(1)	0.0006(1)
D(1)	Expt.	0.0353(6)	0.0439(7)	0.0185(4)	0.0234(6)	−0.0017(5)	−0.0087(5)
	PIMD	0.0438(1)	0.0514(1)	0.0161(1)	0.0317(1)	−0.0030(1)	−0.0091(1)
D(2)	Expt.	0.0184(5)	0.0259(5)	0.0610(8)	0.0046(4)	0.0149(5)	0.0190(5)
	PIMD	0.0163(1)	0.0225(1)	0.0599(1)	0.0020(1)	0.0090(1)	0.0170(1)
D(3)	Expt.	0.0229(5)	0.0165(4)	0.0461(6)	0.0050(4)	−0.0145(4)	−0.0084(4)
	PIMD	0.0212(1)	0.0171(1)	0.0435(1)	0.0029(1)	−0.0146(1)	−0.0032(1)

with very well, will dominate. The C–D corrections are more than 14 times the bond-length uncertainties, demonstrating that they are highly significant.

Table III gives some of the intramolecular interbond and torsion angles in the experimental time-averaged and equilibrium structures. Thermal motion seems to affect the interbond angles only slightly but there are substantial corrections to the torsion angles, which are greater than 30σ. The TLS method is based on an assumption of harmonic curvilinear motion, but it is evident from the torsional corrections that the librational motion of the methyl group is highly anharmonic.

In addition to studying methyl-group rotation, previous interest in nitromethane has also focused on the O···D−C intermolecular hydrogen-bonding interaction.[8] The 15 K experimental structure has a number of short contacts between O atoms and D atoms, some of which are listed in Table IV. The corrections to the distances are large and in every case statistically significant, with values ranging from 10 to 40 times the distance uncertainties. However, the corrections do not alter the conclusions of Jeffrey *et al.*,[8] who used an O···H distance criterion of 2.7 Å, and found that O(1) has four H bonds while O(2) has none. The two different N–O distances also differ by 0.0045(15) Å in the time-averaged experimental structure, further suggesting that they have different intermolecular bonding environments. The MD simulations (and TLS corrections) suggest that this difference is significant with small and similar corrections for these distances (Table II). The presence of such large corrections to intermolecular distances, even at 15 K, shows the pitfalls of ignoring thermal motion effects.

Increasingly, structural studies are focusing on comparing intermolecular distances, particularly for understanding more about the processes of cocrystallization and polymorphism. When precision is essential it is now common to study materials at low temperatures (as was the case with nitromethane, with two reports of crystal structures at 4.2 K and one at 15 K). While going to lower temperatures reduces the effects of thermal motion it does still remain significant. Methyl groups will always be extreme cases, due to the potential for large-amplitude rotations of the groups, but in nitromethane, there are still significant corrections for heavy-atom intermolecular distances. For example, the N···N intermolecular experimental equilibrium distance of r_e^{MD} =4.004(2) Å is 0.024 Å longer in the time-averaged structure r_{ave}^{exp}. More studies, on a wide range of crystal structures, are required to understand the extent of this issue, especially with crystal structures being used to fit force fields and parameterize semi-empirical methods (such as the PM6 method,[38] which used structural information from the Cambridge Structural Database[39]) and also as direct input into computational techniques such as the Pixel method,[40] which uses theoretical calculations to determine lattice and intermolecular binding energies.

TABLE II. Experimental time-averaged bond lengths (in Å) in nitromethane, r_{ave}^{exp}, together with the reported TLS corrections ($\Delta r = r_{TLS} - r_{ave}^{exp}$) and the MD-derived corrections ($\Delta r_{MD} = r_e - r_{ave}^{MD}$). Note that TLS corrected distances were previously reported to only three decimal places with no uncertainties.

	r_{ave}^{exp}	Δr_{TLS}	Δr_{MD}
r[C−N]	1.4855(9)	0.002	−0.0040(9)
r[N−O(1)]	1.2270(9)	0.004	−0.0028(9)
r[N−O(2)]	1.2225(9)	0.002	−0.0014(9)
r[C−D(1)]	1.0751(13)	0.018	0.0159(13)
r[C−D(2)]	1.0736(14)	0.018	0.0183(14)
r[C−D(3)]	1.0739(13)	0.017	0.0144(13)

TABLE III. Selected experimental time-averaged (θ_{ave}^{exp}) bond angles and torsion angles (in degrees) of d_3-nitromethane, together with the experimental equilibrium values (θ_e^{MD}) determined from the experimental equilibrium structure after applying the PIMD-derived position corrections.

	θ_{ave}^{exp}	θ_e^{MD}	$\Delta\theta = \theta_e^{MD} - \theta_{ave}^{exp}$
∠[C−N−O(1)]	118.2(1)	118.1(1)	−0.1
∠[O(1)−N−O(2)]	123.7(1)	123.8(1)	0.1
∠[N−C−D(1)]	107.7(1)	107.4(1)	−0.3
φ[O(1)−N−C−D(1)]	151.7(1)	148.0(1)	−3.7
φ[O(1)−N−C−D(2)]	−89.4(1)	−92.9(1)	−3.5
φ[O(1)−N−C−D(3)]	29.9(1)	26.4(1)	−3.5

TABLE IV. Selected experimental time-averaged intermolecular distances, r_{ave}^{exp}, for d_3-nitromethane, together with the PIMD-corrected experimental equilibrium values, r_e^{MD}. All values are given in Å.

	r_{ave}^{exp}	r_e^{MD}	$\Delta r = r_e^{MD} - r_{ave}^{exp}$	Molecule
r[O(1)···D(1)]	2.386(1)	2.404(1)	0.018	$\frac{1}{2}-x, 2-y, \frac{1}{2}+z$
r[O(1)···D(2)]	2.582(2)	2.572(2)	−0.010	$\frac{1}{2}+x, \frac{3}{2}-y, 1-z$
r[O(1)···D(3)]	2.566(1)	2.605(1)	0.039	$\frac{1}{2}+x, \frac{5}{2}-y, 1-z$
r[O(1)···D(2)]	2.465(2)	2.453(2)	−0.012	$1+x, y, z$
r[O(2)···D(1)]	2.692(2)	2.703(2)	0.011	$-x, -\frac{1}{2}+y, \frac{1}{2}-z$
r[O(2)···D(3)]	2.859(2)	2.779(2)	−0.080	$\frac{1}{2}-x, 2-y, -\frac{1}{2}+z$

2. High-resolution powder neutron diffraction data at 4.2 K

As well as the single-crystal studies highlighted above, the crystal structure of d_3-nitromethane has also been studied a number of times using powder neutron diffraction. The most precise study was performed by David *et al.*[11] using the HRPD machine at the ISIS facility. The large volume of data collected by the HRPD machine allowed for the refinement of ADPs. This study focused on comparing powder diffraction results at 4.2 K with the 15 K single-crystal work of Jeffrey *et al.*[8] To ensure that the comparison was meaningful the same TLS approach that was used for the 15 K data by Jeffrey *et al.*[8]was applied to correct the 4.2 K bond lengths for thermal effects. Table IV compares the MD and TLS-determined equilibrium distances at 4.2 and 15 K. Being able to compare equilibrium structures at two temperatures is very important as the equilibrium structures (particularly bond lengths and angles) should be very similar if the corrections and indeed the experimental structures are correct. The work by David *et al.*[11] found that the single-crystal data were superior and the larger uncertainties in the 4.2 K distances ensure that the data from the two temperatures are in reasonable agreement. It is highly encouraging that differences between the equilibrium geometries at the two temperatures are smaller when the MD corrections are used, in all but one case. The sole discrepancy is in the C–D(1) distance, which has a very small Morse correction compared to D(2) and D(3), which we attribute to the unusual orientation of the experimental thermal ellipsoids/PDFs.

C. Temperature dependence of thermal motion

The simulations described here can also be used to study the temperature dependence of the anharmonic thermal motion in the crystal structure of d_3-nitromethane. In order to quantify the effects of temperature on the atomic position distributions, we examine here the ADPs determined in PIMD simulations.

Figure 4 shows the U_{11} values of the O(1) atom as a function of temperature. The isotropic displacement parameter, U, for a harmonic oscillator is given by[41]

$$U_{harm} = \frac{\hbar}{2\omega m} \times \coth\left(\frac{\hbar\omega}{2k_b T}\right), \tag{11}$$

where ω is the frequency of vibration of the oscillator and m is the associated mass. A fit of this function to U_{11} for O(1) is also shown in Fig. 4. At large values of T, the function is

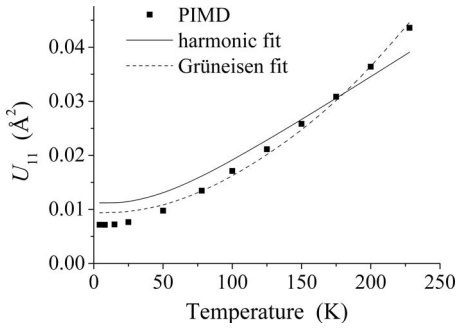

FIG. 4. Temperature dependence of U_{11} (in Å^2) of the O(1) atom in d_3-nitromethane, as determined in PIMD simulations. For comparison, the simple harmonic model of Eq. (11) and the modified harmonic model with effective frequency given by Eq. (12) (the Grüneisen fit) are also shown.

effectively linear while, as $t \to 0$, it approaches a finite value due to the ZPE contribution to the motion. Deviations from the ideal harmonic behavior were defined by Bürgi *et al.*[41] as "positive anharmonicity" (when the thermal motion increases faster than the harmonic behavior would suggest) and "negative anharmonicity" (when the thermal motion increases slower than the harmonic behavior). At higher temperatures, more of the free-energy surface is explored. Thus positive anharmonicity represents a broadening of the free-energy surface away from the equilibrium point while a steeper surface is implied in the case of negative anharmonicity. Figure 4 clearly demonstrates that the dynamics of the O(1) atom exhibit positive anharmonicity. The numerical PDFs, calculated from the PIMD simulations, show nearly Gaussian distributions for the O atoms at low temperatures but, as Fig. 5 shows, the distributions become asymmetric at higher temperatures.

One approach to correcting the harmonic model ADPs for such temperature-dependent anharmonicity is to substitute an effective frequency, $\omega_{eff}(T)$, in Eq. (11). The effective frequency can be defined by a Grüneisen parameter, γ,[41]

$$\omega_{eff}(T) = \omega\left[1 - \gamma\left(\frac{V(T) - V_{min}}{V_{min}}\right)\right], \tag{12}$$

where V is cell volume and V_{min} is the volume at the lowest experimental temperature. The volume term is equivalent to the thermal expansion coefficient, χ_T. This approach is re-

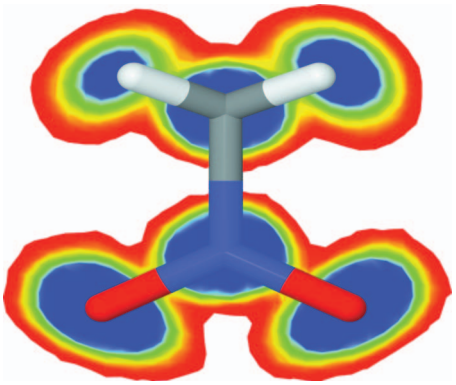

FIG. 5. Two-dimensional slice through the numerical PDFs of d_3-nitromethane at 228 K. The NO_2 fragment is in the plane of the paper, and probability density increases from red to blue.

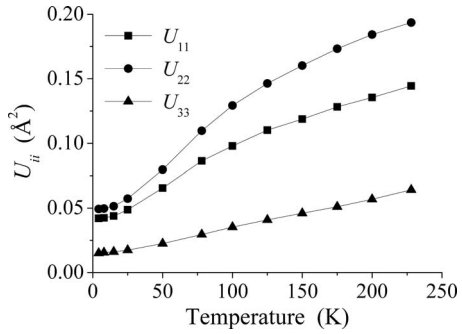

FIG. 6. U_{ii} values (in Å^2) of the D(1) atom in d_3-nitromethane at temperatures between 4.2 and 228 K, as determined in PIMD simulations.

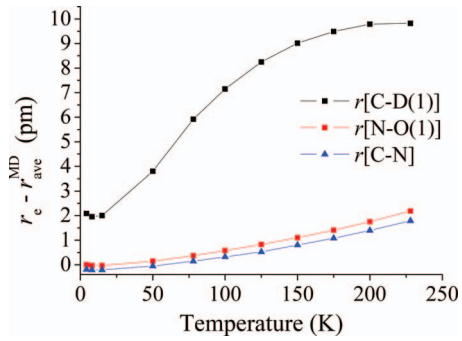

FIG. 8. PIMD distance corrections ($r_e - r_{ave}^{MD}$; in pm) to r[C–D(1)], r[N–O(1)], and r[C–N] at temperatures between 4.2 and 228 K.

ferred to as a quasiharmonic model. Equation (11), with the effective frequency given by Eq. (12), was used to fit the calculated U_{11} values of the O(1) atom. The thermal expansion χ_T was fitted to the function $a_1T+a_2T^2$ after Schwarzenbach *et al.*[42] and the harmonic frequency ω was treated as a fitting parameter. The dashed line in Fig. 4 represents the quasiharmonic fit, which models the temperature dependence significantly better than the harmonic model, although a multifrequency model would be expected to yield an even better fit. This fitting procedure gives a value of 3.0(5) for the Grüneisen parameter. We note that this value is consistent with the work of Bürgi *et al.*,[41] who analyzed the temperature dependence of the ADPs of hexamethylenetetramine (HMT) by treating the molecule as a rigid body. In that case, values for γ of between 2.3 and 5.3 were determined for a variety of models applied to the ADPs of HMT at temperatures ranging from 15 to 298 K.

In contrast to the oxygen atoms, the deuterium atoms' ADPs (the U_{ii} values for D(1) are plotted in Fig. 6) show negative anharmonicity. There is an upper limit on the size of ADPs due to the pseudoaxis of symmetry of the deuterium atoms. The U_{33} value of D(1) follows the linear high-temperature behavior predicted by the harmonic model, which is an indication that the anharmonicity is primarily in the x and y directions. This makes sense in terms of the orientation of the D(1) atom and the axis of rotation. The numerical PDFs depicted in Fig. 7 show how the harmonic model of three separate atoms is far from reality. Our simulations predict significant deviations from the trivariate Gaussian behavior, clearly demonstrating the importance of anharmonicity.

Figure 8 shows the bonded distance corrections as a function of temperature, as determined in PIMD simulations. The sampling uncertainties in the distance corrections are typically less than 0.1 pm. The C–D corrections rise to very large values of ~0.1 Å. As we see in Fig. 8 (and Table II), the usual effect of librational motion of a molecule is to shorten the time-averaged intramolecular bond lengths.[2] As we might expect from the D(1) ADP behavior, the C–D(1) the correction begins to plateau at higher T. In contrast, the smaller C–N and N–O(1) corrections continue to rise. This is consistent with the concept of positive anharmonicity, where the free-energy surface appears more anharmonic as the temperature rises. Closer inspection of Fig. 8 shows that, at low temperatures, the time-averaged lengths of the C–N and N–O(1) bonds are longer than their equilibrium values (i.e., the distance correction $r_e - r_{ave}^{MD}$ is negative) (Table V). The bond stretches are modeled using Morse potentials and, for an isolated diatomic molecule, such an asymmetric potential results in a time-averaged bond length longer than the equilibrium length as the temperature increases. The initial decrease of the distance corrections in Fig. 8 is the result of this lengthening effect competing with the usual librational shortening behavior. However, we find that this effect is quite small and only present at the lowest temperatures.

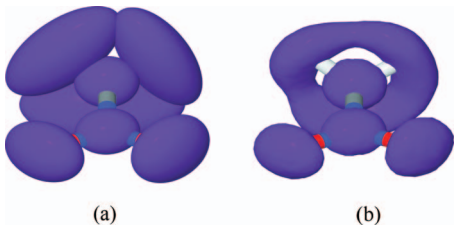

FIG. 7. Isosurface of (a) the trivariate Gaussian PDFs and (b) numerical atomic PDFs from the PIMD simulation of d_3-nitromethane at 228 K. The harmonic isosurface is plotted at the 90% probability level. The numerical isosurface has been chosen so that the N-atom isosurfaces are similar in both plots.

IV. CONCLUSION

A series of classical MD and quantum PIMD simulations have been performed on d_3-nitromethane at temperatures ranging from 4.2 to 228 K. The results compare favorably to the existing low-temperature neutron-diffraction data sets. In particular, the experimental equilibrium structures have been determined at 4.2 and 15 K. The corrections to atomic positions are large in magnitude, ranging from 0.02 to 0.1 Å at 15 K. As a result, corrections to C–D distances, intermolecular distances, and torsions are large and statistically significant, highlighting the importance of including anharmonic thermal motion effects in diffraction studies.

The use of PIMD simulations has been important for determining the distance corrections at low temperatures, where classical MD fails to capture the effects of quantum fluctuations in the atomic positions. A comparison was made between the full PIMD simulations and an approximation based on the work of Feynman and Hibbs,[28] which has been used a number of times for liquid simulations. The FH approximation overestimates the swelling effect in the quantum

TABLE V. Equilibrium bond distances, r_e^{MD}, obtained by applying the corrections derived from PIMD simulations to the time-averaged experimental structure at 4.2 and 15 K. The bond lengths determined by applying TLS corrections are also shown for comparison. The final two columns show the differences between the final equilibrium bond distances as determined by applying PIMD-derived or TLS corrections. All distances are given in Å.

	4.2 K		15 K			
	r_e^{MD}	r_{TLS}	r_e^{MD}	r_{TLS}	Δr[a]	Δr_{TLS}[b]
r[C–N]	1.4803(27)	1.4867	1.4815(9)	1.4887	0.0012	0.0020
r[N–O(1)]	1.2294(29)	1.2402	1.2242(9)	1.2309	−0.0052	−0.0093
r[N–O(2)]	1.2237(31)	1.2318	1.2211(9)	1.2253	−0.0026	−0.0065
r[C–D(1)]	1.0809(38)	1.0926	1.0910(14)	1.0911	0.0101	−0.0015
r[C–D(2)]	1.0880(41)	1.0838	1.0922(14)	1.0929	0.0042	0.0091
r[C–D(3)]	1.0877(37)	1.0858	1.0883(14)	1.0908	0.0006	0.0050

[a] $\Delta r = r_e^{MD}(15\ K) - r_e^{MD}(4.2\ K)$.
[b] $\Delta r_{TLS} = r_{TLS}(15\ K) - r_{TLS}(4.2\ K)$.

regime. This is clearly a result of the presence of significant intra- and intermolecular forces in the solid state, which reduce the "quantum swelling" of the atomic distributions.

The temperature dependence of the ADPs and corrections has also been explored. The ADPs deviate significantly from the ideal behavior expected for harmonic oscillators. It has been shown that a simple quasiharmonic model can reproduce the temperature dependence adequately. The deviations can be correlated with the numerical PDFs and distance corrections. In studying nitromethane, the MD method has been applied to the important class of methyl groups, which are the classical example of curvilinear, anharmonic motion. The numerical PDFs should provide useful insights for the design and assessment of new anharmonic structure factor equations.

ACKNOWLEDGMENTS

The PIMD simulations were performed using the resources of the EaStCHEM Research Computing Facility (http://www.eastchem.ac.uk/rcf). This facility is partially supported by the eDIKT initiative (http://www.edikt.org.uk). We thank Dr. Richard Ibberson for useful discussions and Professor David Manolopoulos for a review of a draft manuscript. A.M.R. acknowledges the School of Chemistry, University of Edinburgh for funding a studentship, C.A.M. acknowledges the Royal Society for the award of a University Research Fellowship, and S.H. acknowledges the U.S. Office of Naval Research for funding under Contract No. N000140510460.

[1] A. Katrusiak, Acta Crystallogr. A: Found. Crystallogr. **64**, 135 (2008).
[2] D. W. J. Cruickshank, Acta Crystallogr. **9**, 757 (1956).
[3] V. Schomaker and K. N. Trueblood, Acta Crystallogr. B: Struct. Crystallogr. Cryst. Chem. **24**, 63 (1968).
[4] W. F. Kuhs, Acta Crystallogr. A: Found. Crystallogr. **48**, 80 (1992).
[5] C. Scheringer, Acta Crystallogr. A: Found. Crystallogr. **42**, 356 (1986).
[6] A. M. Reilly, D. A. Wann, C. A. Morrison, and D. W. H. Rankin, Chem. Phys. Lett. **448**, 61 (2007).
[7] D. A. Wann, A. V. Zakharov, A. M. Reilly, P. D. McCaffrey, and D. W. H. Rankin, J. Phys. Chem. A **113**, 9511 (2009).
[8] G. A. Jeffrey, J. R. Ruble, L. M. Wingert, J. H. Yates, and R. K. McMullan, J. Am. Chem. Soc. **107**, 6227 (1985).
[9] R. Ouillon, J.-P. Pinan-Lucarré, and P. Ranson, J. Chem. Phys. **116**, 4611 (2002).
[10] C. C. Wilson, Crystallogr. Rev. **13**, 143 (2007).
[11] W. I. F. David, R. M. Ibberson, G. A. Jeffrey, and J. R. Ruble, Physica B **180–181**, 597 (1992).
[12] S. F. Trevino, E. Prince, and C. R. Hubbard, J. Chem. Phys. **73**, 2996 (1980).
[13] S. F. Trevino and W. H. Rymes, J. Chem. Phys. **73**, 3001 (1980).
[14] A. Heidemann, I. Anderson, B. Jeffryes, and B. Alefeld, Z. Phys. B: Condens. Matter **49**, 123 (1982).
[15] D. T. Cromer, R. R. Ryan, and D. Schiferl, J. Phys. Chem. **89**, 2315 (1985).
[16] M. Citroni, F. Datchi, R. Bini, M. Di Vaira, P. Pruzan, B. Canny, and V. Schettino, J. Phys. Chem. B **112**, 1095 (2008).
[17] L. Zheng, S.-N. Luo, and D. L. Thompson, J. Chem. Phys. **124**, 154504 (2006).
[18] D. C. Sorescu, B. M. Rice, and D. L. Thompson, J. Phys. Chem. B **104**, 8406 (2000).
[19] E. F. Byrd, G. E. Scuseria, and C. F. Chabalowski, J. Phys. Chem. B **108**, 13100 (2004).
[20] M. W. Conroy, I. I. Oleynik, S. V. Zybin, and C. T. White, J. Phys. Chem. A **113**, 3610 (2009).
[21] S. J. Grimme, J. Comput. Chem. **25**, 1463 (2004).
[22] E. W. Draeger and D. M. Ceperley, Phys. Rev. B **61**, 12094 (2000).
[23] D. C. Sorescu, B. M. Rice, and D. L. Thompson, J. Phys. Chem. B. **101**, 798 (1997).
[24] M. P. Allen and D. J. Tildesley, *Computer Simulation of Liquids* (Oxford University Press, New York, 1989).
[25] It should be noted that the harmonic bending constants given in the original paper were incorrect; the values reported by Agrawal *et al.* (Ref. 26) have been used instead.
[26] P. M. Agrawal, B. M. Rice, and D. L. Thompson, J. Chem. Phys. **119**, 9617 (2003).
[27] H. C. Andersen, J. Chem. Phys. **72**, 2384 (1980).
[28] R. P. Feynman and A. R. Hibbs, *Quantum Mechanics and Path Integrals* (McGraw-Hill, New York, 1965).
[29] M. Parrinello and A. Rahman, J. Chem. Phys. **80**, 860 (1984).
[30] M. E. Tuckerman, *Path Integration via Molecular Dynamics*, Quantum Simulations of Complex Many-Body Systems: From Theory to Algorithms, Lecture Notes–NIC Series Vol. 10 (John von Neumann Institute for Computing, Jülich, 2002).
[31] T. E. Markland and D. E. Manolopoulos, J. Chem. Phys. **129**, 024105 (2008).
[32] T. E. Markland and D. E. Manolopoulos, Chem. Phys. Lett. **464**, 256 (2008).
[33] T. Pilati, F. Demartin, and C. M. Gramaccioli, Phys. Chem. Miner. **26**, 149 (1998).
[34] G. A. Voth, Phys. Rev. A **44**, 5302 (1991).
[35] B. Guillot and Y. Guissani, J. Chem. Phys. **108**, 10162 (1998).
[36] T. E. Markland, S. Habershon, and D. E. Manolopoulos, J. Chem. Phys. **128**, 194506 (2008).
[37] C. K. Johnson, *Thermal Neutron Diffraction* (Oxford University Press, New York, 1970).

[38] J. J. P. Stewart, J. Mol. Model. **13**, 1173 (2007).
[39] F. H. Allen, Acta Crystallogr. B: Struct. Crystallogr. Cryst. Chem. **58**, 380 (2002).
[40] A. Gavezzotti, Z. Kristallogr. **220**, 499 (2005).
[41] H. B. Bürgi, S. C. Capelli, and H. Birkedal, Acta Crystallogr. A: Found Crystallogr. **56**, 425 (2000).
[42] D. Schwarzenbach, H. Birkedal, M. Hostettler, and P. Fischer, Acta Crystallogr. B: Struct. Crystallogr. Cryst. Chem. **63**, 828 (2007).